文章编号:1671-8879(2017)04-0001-11

Calculation model of permafrost table of XPS insulated board subgrade in warm permafrost regions

TAI Bo-wen[1], LIU Jian-kun[1,2], FANG Jian-hong[2], XU An-hua[2], LIU Lei[2], WANG Teng-fei[1]

(1. School of Civil Engineering, Beijing Jiaotong University, Beijing 100044, China; 2. Key Laboratory of Highway Construction & Maintenance Technology in Permafrost Region, Qinghai Research Institute of Transportation, Xining 810008, Qinghai, China)

Abstract: In order to reveal the decline laws of permafrost table of expressway subgrades in warm frozen soil regions of Qinghai-Tibet Plateau, ensure the long-term thermal stability of subgrades in warm permafrost regions and reduce subgrade diseases which caused by the degradation of artificial permafrost table, firstly, the longitudinal and lateral distributions of ground temperature of XPS insulated board subgrade and degradation characteristics of artificial permafrost table at early stage of subgrade construction were analyzed. Secondly, the moisture-heat coupling differential equation of permafrost was solved through unsaturated soil seepage and heat transfer theory, to realize the unity coupling of moisture field and temperature field of frozen soils. The temperature field simulated by moisture-heat model was compared with the measured temperature field to verify the correctness of the model. Then, the degradation laws of artificial permafrost table of XPS insulated board subgrade under five conditions (filling type, annual mean ground temperature, height of subgrade, laying location of XPS thermal insulation board and climate warming) were analyzed. Finally, main factors influencing the degradation of artificial permafrost table were calculated by MATLAB, and the multivariate linear regression was carried out, so as to establish the calculation model for artificial permafrost table of XPS insulated board subgrade in warm permafrost regions. The results show that temperatures on the left side of XPS insulated board subgrade is higher than that on the right side within a certain range. The artificial permafrost table lifts 60 cm at the early stage of subgrade construction, then, decreases gradually with a speed of 10 cm per year. The change of permafrost table leads to a certain increase of temperature in deep permafrost. Under the five conditions, the artificial permafrost table of XPS insulated board subgrade in warm permafrost regions increases linearly with time. Filling type and climate warming are two major factors affecting the decline of permafrost table. The model can provide favorable references for prediction and prevention of long-term deformation of highway subgrades in warm permafrost regions. 4 tabs, 10 figs, 25 refs.

Key words: road engineering; calculation model of permafrost table; numerical calculation; Gonghe-Yushu Expressway

CLC number: U416.168 **Document code**: A

Received date: 2017-02-21

Author resume: TAI Bo-wen(1988-), male, PhD Candidate, E-mail:taibw@qq.com.

Corresponding author: LIU Jian-kun(1965-), male, Professor, Doctoral tutor, E-mail:jkliu@bjtu.edu.cn.

高温冻土区 XPS 保温板路基的冻土上限计算模型

邰博文[1],刘建坤[1,2],房建宏[2],徐安花[2],刘 磊[2],王腾飞[1]

(1. 北京交通大学 土木建筑工程学院,北京 100044; 2. 青海省交通科学研究院 多年冻土地区公路建设与养护技术交通行业重点实验室,青海 西宁 810008)

摘 要:为揭示青藏高原东部高温冻土区高速公路 XPS 保温板路基的人为冻土上限退化规律,确保高温冻土区路基的长期热稳定性,减小因人为冻土上限退化引起的路基病害,首先,利用现场地温实测资料分析高温冻土区 XPS 保温板路基地温的纵、横向分布特征,以及路基修筑初期人为冻土上限的退化特征;然后,采用非饱和土渗流与热传导理论求解冻土水热耦合微分方程,实现冻土水分场与温度场的全耦合,进而将水热耦合模型模拟所得温度场与现场实测温度场进行比较,以验证该模型的正确性;并分析 XPS 保温板路基在 5 种工况(包括填料类型、年平均地温、路基高度、XPS 保温板铺设位置和气候变暖)下人为冻土上限的退化规律;最后,采用 MATLAB 分析影响人为冻土上限退化主要因素,进而对其进行多元线性回归,建立高温冻土区 XPS 保温板路基人为冻土上限计算模型。研究结果表明:XPS 保温板路基左侧一定范围内温度比右侧对应范围的温度高;路基修筑初期人为冻土上限先抬升 60 cm,然后以 10 cm/年下降,冻土上限的变化导致深部冻土层存在一定幅度的升温;5 种工况条件下,路基人为冻土上限与时间均呈线性增加关系;影响人为冻土上限退化的 2 个主要影响因素为填料类型和气候变暖;该模型可为今后开展高温冻土区高速公路 XPS 保温板路基长期变形预测与病害防治提供技术参考。

关键词:道路工程;冻土上限计算模型;数值计算;共和—玉树高速公路

0 Introduction

According to the freezing time of soils and rocks, the frozen soil can be divided into three categories. One of these categories is known as permafrost soil which has been in a continuously frozen state for more than two years. The second one is called seasonal frozen ground, which means that only the surface layer of the soil (up to several meters below the ground surface) thaws in summer and freezes in winter. The third one is called short-term frozen soil whose existing time only extends to a few hours, or a couple of days. Permafrost in China is mainly distributed in Qinghai-Tibet Plateau and Greater Khingan Mountains. Subgrades of highways in these areas will be affected by damages such as thawing settlement and strength variation, which greatly influence the safety and comfort of driving. Building subgrade in these places will mainly face to long-term thaw settlement, which is mainly caused by the decline of permafrost table. In order to prevent the decline of permafrost table, many domestic and international scholars have studied the application of XPS insulated board subgrade to cool the foundation.

Tai, et al. analyzed the distribution features of ground temperature of XPS insulation embankment test section in Maduo site of Gonghe-Yushu Expressway[1]. Based on the observed data of insulation embankment test section in Beiluhe site of Qinghai-Tibet Railway, Sheng, et al. analyzed the dynamic process of underlying permafrost, and temperature accumulation at both surfaces of insulation layer. The results show that the insulation embankment has the function of protecting permafrost; the heat entering insulation layer presents a serious asymmetry; and the sunshiny side of embankment absorbs much more heat than that of the shade side[2]. Wen, et al. carried out a series of uniaxial compression test for the production of different manufacturers XPS insulated board, and the elastic modulus and compressive strength of XPS insulated board of different manufacturers were obtained[3]. It is recommended that the road with XPS insulated board should also meet the following two conditions: the elastic modulus should be

greater than 45 MPa, and the compressive strength should be not less than 500 kPa[4]. Hou, et al. used ABAQUS finite element software to simulate the temperature field of expanded polystyrene (EPS) thermal insulation roadbed in permafrost region, and concluded that the thermal insulation materials in roadbed had obvious protective effect on the permafrost under the pavement, and EPS was recommended to be laid at the bottom of the embankment[5]. Based on the permafrost investigation and ground temperature monitoring data for National Highway 214, engineering geological model for evaluating permafrost conditions was established by Chen, et al., and found that evaluation results based on the model for National Highway 214 were similar to the field disease investigation, and the evaluation could effectively guide the operation and maintenance of National Highway 214 and the construction of Gonghe-Yushu Expressway[6]. In order to deal with the applicability and limitation of embankment adjustment measure in permafrost regions, reply to global warming and meet the requirement of expressway construction, six types of general embankment adjustment measures were systematically evaluated by Liu, et al., and four new types of embankment structures were presented by means of mechanism complementation and optimizing design parameter and applied in entity engineering[7-8]. For the severe challenges of global warming, Cheng, et al. put forward measures to actively protect the permafrost, which was cooling the foundation to ensure the stability of the project[9-10]. Niu, et al. implemented long-term in-situ temperature monitoring for ordinary embankment, block stones embankment, embankment with crushed-stone side-slope and U-type block stones embankment, the monitoring results show that these measures can effectively lift the upper limit of permafrost, protect the stability of the embankment[11]. Zhang, et al. adopted the finite element method to make a nonlinear analysis of temperature field of the embankment with crushed-rock revetment and insulation along the Qinghai-Tibet Railway, and it was proposed that in warmer permafrost regions, the insulation should be used to increase the cooling effect of embankment with crushed-rock revetment[12]. Using the working principle of XPS insulated board subgrade, Ma, et al. carried out on-site observations on the IBE test subgrade of Qinghai-Tibet Railway and concluded that the decrease of ground temperature in lower part of the insulating material was served to protect the permafrost table. Based on temperature monitoring data of Qinghai-Tibet Highway in Kunlun Mountains insulation material test section, the numerical results indicated that the embankment with insulation and thermosyphon had advantages of insulation and thermosyphon, for better protection of the permafrost[13]. Liu, et al. implemented numerical analysis for the ventilated embankment with thermal insulation layer in Qinghai-Tibet Railway[14-16]. Tai, et al. applied 2D finite element analysis to conduct XPS insulated board subgrade on warm permafrost zone of Tibet. By changing working conditions, a series of finite element simulations were carried out. The simulated thermal states of XPS insulated board subgrade for different years were presented and discussed, and main influencing factors were outlined[17].

Gonghe-Yushu Expressway is the first expressway in Qinghai-Tibet Plateau permafrost regions, and compared with the existing ordinary highway, this expressway has a higher requirement on subgrade deformation and service life. In order to predict the long-term thaw settlement of the road subgrade, the main reference indexes (degradation rate of permafrost table) leading to the thaw settlement of subgrade need to be calculated exactly. Therefore, by making a comparison between measured temperature field of the subgrade with XPS insulated board and simulated field obtained through moisture-heat coupling model, the paper verified the simulation correctness of the model. Then calculated the changing features of permafrost table of subgrade over time under different working conditions through the model. Besides, with the application of entropy weight method, it was obtained that the filling type of subgrade

and the climate warming are the two major factors affecting the decline of permafrost table, which are the basis for the establishment of calculation model of permafrost table. The model would provide references for a more exact prediction of long-term thaw settlement of subgrade in permafrost regions as well as for a better guidance of traffic departments to prevent subgrade diseases.

1 Calculating principle and model establishment

1.1 Control equation of temperature field

Water migration and redistribution in soils are correlated with heat flow and temperature distribution. With consideration for moisture-thermal coupling problems in the freeze-thaw process, a heat conduction equation was established with the latent heat of phase change as the inner heat sources[18]. The equation is expressed as

$$\rho C_{vs}\frac{\partial T}{\partial t}=\lambda\nabla T^2+L\rho_I\frac{\partial\theta_I}{\partial t} \tag{1}$$

where ρ and ρ_I are densities of soil and ice(kg/m^3), respectively; C_{vs} and λ are effective volumetric heat capacity [J/(kg·℃)] and effective thermal conductivity [W/(m·℃)] of soils changing with temperature; θ_I is volumetric ice content (%); L is the latent heat of phase change (335 kJ/kg); T is temperature (℃); t is time (s).

Taking into account that the water in soil is composed of pore ice and pore water, volumetric water content of frozen soil can be defined as

$$\theta=\theta_u+\rho_I\theta_I/\rho_w \tag{2}$$

where θ is volumetric water content; θ_u is volumetric content of unfrozen water; ρ_w is water density.

1.2 Control equation of water field

Unfrozen water exists throughout the freeze-thaw process. In accordance with the Richards equation of the phase change[19], as well as considering the ice resistance in the freezing process, the water migration equation of unsaturated frozen soil can be expressed by

$$\frac{\partial\theta_u}{\partial t}+\nabla(-D(\theta_u)\nabla\theta_u-k_{g(\theta_u)})+\frac{\rho_I}{\rho_w}\frac{\partial\theta_I}{\partial t}=0 \tag{3}$$

Water diffusivity equation in soil is defined as

$$D=IK/C \tag{4}$$

where D and K are the water diffusivity (%) and the permeability coefficient (m/s) of unsaturated frozen soil, respectively; C is water capacity; $k_{g(Q_u)}$ is the permeability coefficient (m/s) of unsaturated soil in the direction of gravitational acceleration; I is resistance coefficient, which indicates the effect of ice on the water migration in frozen soil, it can be calculated by the following formula

$$I=10^{10\theta_I} \tag{5}$$

1.3 Unfrozen water content

In the freezing process, the free water in soil begins to freeze at a certain temperature below 0 ℃, which is called the initial freezing temperature. Xu, et al. put forward the empirical formula of unfrozen water content through laboratory tests[20]

$$\frac{w_0}{w_u}=\left(\frac{T}{T_f}\right)^b \tag{6}$$

where w_0 is the initial moisture content (%); w_u is the unfrozen water content (%); T_f is the initial freezing temperature (℃); b is a parameter which is related to salt content and soil type and can be determined by either using the one-point method mentioned by Xu et al.[20], or by using experience value 0.58 for silty sand and 0.65 for sandy gravels, respectively.

Bai, et al. put forward the solid phase rate[21]

$$B_I=\frac{\theta_I}{\theta_u}=\begin{cases}1.1\left(\dfrac{T}{T_f}\right)^b-1.1 & T<T_f\\ 0 & T\geqslant T_f\end{cases} \tag{7}$$

where the constant 1.1 refers to the density ratio of water to ice in soil (ρ_w/ρ_I); B_I is solid phase rate, a single-valued function of temperature according to Eq.(7).

To sum up, the coupled equations of water-heat of frozen soil are proposed by using simultaneous temperature field differential Eq.(1), the water field differential Eq.(2) and phase change dynamic equilibrium Eq.(7).

1.4 Establishment of moisture-thermal coupling model of frozen soils based on COMSOL

Eq.(1) and Eq.(3) are transformed into the coefficient partial differential equations provided by

COMSOL

$$\begin{cases}\rho C_{vs}\dfrac{\partial T}{\partial t}+\nabla(-\lambda\nabla T)=L\rho_I\dfrac{\partial\theta_I}{\partial t}\\ \dfrac{\partial\theta_u}{\partial t}+\nabla(-D\nabla\theta_u-k_{g(\theta_u)})+\dfrac{\rho_I}{\rho_w}\dfrac{\partial\theta_I}{\partial t}=0\end{cases}\tag{8}$$

2　Ground temperature measured and model validation

2.1　Features of measured ground temperature

2.1.1　Descriptions of filed monitoring site

The Gonghe-Yushu Expressway, simply called GYE, is the first expressway with a total length of 634.8 km in Qinghai-Tibet Plateau, China. 227.7 km of the expressway is laid on the permafrost, most of which is high temperature unstable permafrost whose annual average ground temperature is higher than −1 ℃. It starts at Gonghe County (100°33′E, 36°19′N) and ends at Yushu County (97°01′E, 33°08′38″N). It passes through, Heka Mountain, Ela Mountain, Changshitou Mountain and Bayan Har Mountain.

To investigate long-term stability of embankment, a long-term monitoring system of ground temperature was installed along the GYE in permafrost regions. The observation site at section K423+500, lies between Changshitou Mountain to Maduo County along the GYE on Qinghai-Tibet Plateau, belonging to the alpine steppe climate. The height is about 4 300 m above the sea level. The vegetation coverage is about 50%. The average annual air temperature varies from about −3.3 ℃ to −4.1 ℃. The annual extreme high and low air temperatures are 18 ℃ and −26.6 ℃, respectively. The annual precipitation is up to 310 mm. The maximum wind speed is 34 m/s and the annual average wind speed is 3.2 m/s. According to drilling survey, the permafrost table is about 2.3 m and the mean annual ground temperature is 0.98 ℃. The type of permafrost is warm instable permafrost. The ground is mainly composed of sandstone, fine sand and silty sand.

2.1.2　Section and method for observation

Fig. 1 shows the monitoring sections of the test subgrade with XPS insulated board. The embankment height is 2.2 m and the filling material is sandy gravels. The width of subgrade surface is 10 m and the slope ratio is 1∶1.5. XPS insulated board is laid below the subgrade surface at a distance of 80 cm. The longitudinal and horizontal temperature measurement sensors are installed at monitoring section. The longitudinal temperature measurement sensors are embedded in shoulders, toes of slope, subgrade center and natural ground with a hole depth of 15 m, which are designed at the intervals of 0.5 m (from 0 to 5 m), and of 1.0 m from 5 to 15 m. Horizontal temperature measurement sensors are embedded on the top and under surfaces of XPS insulated board, embedded at the interval of 1 m along the subgrade section. The observation frequency is once at every 5 days. This study adopted ground temperature data from July 2013 to July 2014, which included one whole freeze-thaw cycle. The construction process of subgrade with XPS insulated board is presented in Fig. 2.

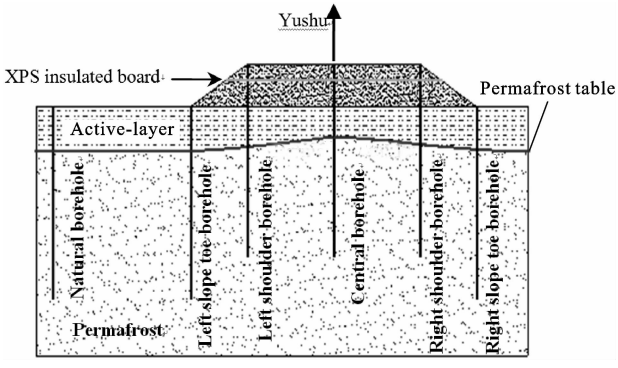

Fig. 1　Monitoring section of subgrade XPS insulated board subgrade

图 1　XPS 保温板路基的监测断面

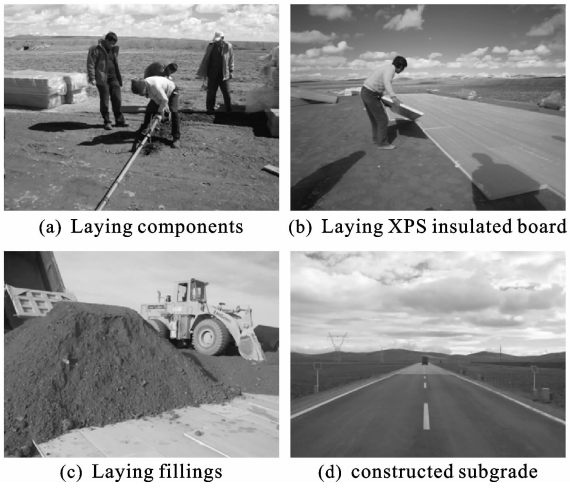

(a) Laying components　(b) Laying XPS insulated board

(c) Laying fillings　(d) constructed subgrade

Fig. 2　Construction process of XPS insulated board subgrade

图 2　XPS 保温板路基的修筑过程

2.1.3 Field ground temperature

(1) Lateral distribution of ground temperature

Fig. 3 indicates the lateral distribution of ground temperature of subgrade with XPS insulated board on July 21st, 2014, which is the highest temperature period of the natural environment in this region. Around the center of subgrade with XPS insulated board, the temperature at the top of the board is 13 ℃ higher than that on the bottom while temperature on the bottom at the moment is 4 ℃. Besides, temperature of the embankment in time remains above 0 ℃, which suggests that the outside warm air has obviously thermal effects on the fillings of subgrade, leading to unfavorably conditions for subgrade in warm seasons.

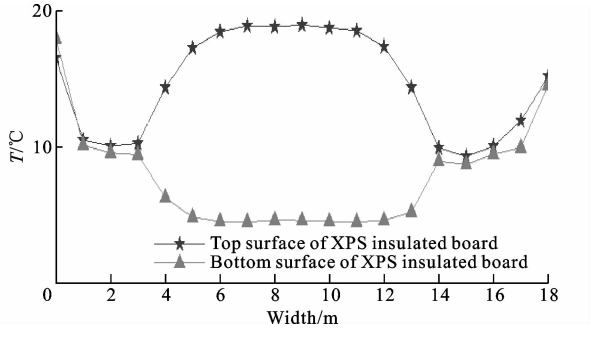

Fig. 3 Lateral temperature distribution curves of subgrade (July 21st, 2014)

图 3 路基横向温度分布曲线(2014 年 7 月 21 日)

Fig. 4 shows the lateral distribution of ground temperature of subgrade with XPS insulated board on January 16th, 2014, which corresponds to the lowest temperature of natural environment in the region. At the center of subgrade with XPS insulated board, temperature on top of the board is about 5 ℃ lower than the bottom and temperature of the bottom at the moment is −2.5 ℃. Meanwhile, temperature of the embankment is generally below 0 ℃, indicating that the lower temperature inside the subgrade in cold seasons has a cooling effect on the underlying permafrost.

From Fig. 3 and Fig. 4, it can be concluded that temperature on the left side of the subgrade within a certain range is higher than that on the right side, within the corresponding range both in cold and warm seasons, which proves that after building the embankment, ground temperature distribution of the subgrade varies greatly between the south-faced slope and the north-faced slope, as a result of slope orientations and different boundary conditions, such as surface turbulence and solar radiation.

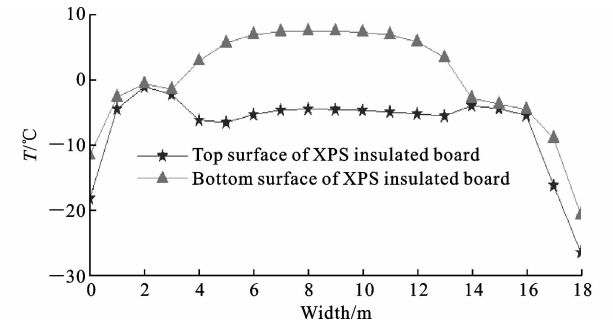

Fig. 4 Lateral temperature distribution curves of subgrade (January 16th, 2014)

图 4 路基横向温度分布曲线(2014 年 1 月 16 日)

(2) Vertical distribution of ground temperature

Fig. 5 shows that the inter-annual change features of ground temperature of subgrade center at different depths H. They are presented in cosine curves with roughly the same cycle as ground temperature. With the increase of depth, and the change amplitude of the ground temperature decreases, and the phase of the ground temperature is relatively delayed. In addition, annual temperature difference of each measuring point decreases with the increase of depth, and the main reason is the effect of external factors, such as solar radiation, wind direction, wind force, ground snow, etc., on the temperature of subgrade, which decreases gradually with the increase of depth. At a certain depth, the annual change curve of ground temperature will become closer to a straight line, which means that the soil reaches a thermally stable state.

Fig. 6 presents the changes of permafrost table at the subgrade center, in which the distribution of ground temperatures over depths are counted from the natural ground surface. Fig. 6 shows that the permafrost table is lifted with the uplift amplitude of about 0.4 m at the early stage of the subgrade completion while within a certain depth range below the permafrost table, temperature of frozen soils increases. In the second year after the subgrade is completed, the permafrost table declines

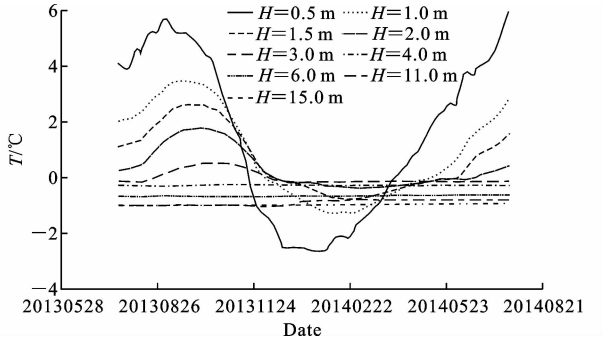

Fig. 5　Changes of ground temperature with different depths in subgrade center

图 5　路基中心不同深度地温的变化

with an amplitude of about 0.07 m, but the temperature of underlying permafrost continues to show an increasing trend. To sum up, changes of artificial permafrost table of subgrade will consume the cold-storing quantities of underlying permafrost against the background of global warming.

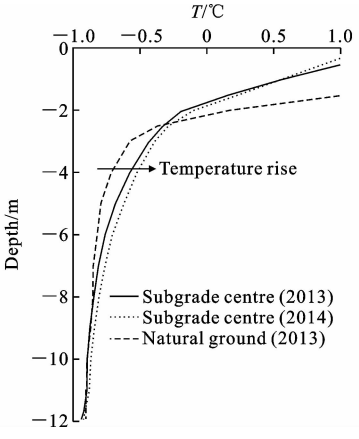

Fig. 6　Position of permafrost table

图 6　冻土上限的位置

2.2　Moisture-thermal coupling model validated

2.2.1　Geometric model and physical parameters

In order to verify the moisture-thermal coupling model established in this paper, the following section adopts a moisture-thermal coupling model based on the secondary development of COMSOL to simulate the changing features of temperature field of XPS insulated board embankment test section in Maduo site of Gonghe-Yushu Expressway. Physical parameters of different soil layers of subgrade are summarized in Tab. 1. The numerical model is established as shown in Fig. 7 and the specific geometrical dimensions are as follows: the surface width of the subgrade is 10.0 m; its bottom width is 16.6 m, with the height of 2.2 m; and the slope gradient is 1∶1.5. XPS insulated board is laid in the depth of 80 cm under the pavement, the thickness of XPS insulated board is 8 cm.

2.2.2　Simulation process and model validation

In the background of global warming and the temperature rising 2.6 ℃ within 50 years, this paper simulated the variation features of temperature field of subgrade built 2 years later. The water boundary of the subgrade is set as constant, there is no external water supply, and water content of the subgrade soil is the initial water content. The thermal boundary conditions of the numerical simulation are as follows: according to field monitoring results, thermal boundary condition of the bottom of the model is set as the temperature value of −1 ℃. The first thermal boundary condition is adopted at the upper boundary of the model, expressed with a cosine function shown in Eq. (9). The parameters in Eq. (9) is obtained by fitting the measured ground temperature from 2013 to 2014. The fitting parameters are shown in Tab. 2

$$T=T_0+0.052t/365+A\sin(2\pi t/365+\varphi\pi) \quad (9)$$

where T_0 is the mean annual temperature (℃); A is the temperature amplitude; φ is the initial phase temperature.

Firstly, with no subgrade having been built yet, temperature field of the soil after 50 years was calculated, and upper thermal boundary was set as thermal boundary of the natural ground surface ac-

Tab. 1　Physical parameters in different soil layers

表 1　不同土层的物理参数

Parameters	D/m	ρ/(kg·m^{-3})	C_f/(J·kg^{-1}·℃$^{-1}$)	C_u/(J·kg^{-1}·℃$^{-1}$)	λ_f/(W·m^{-1}·℃$^{-1}$)	λ_u/(W·m^{-1}·℃$^{-1}$)
Sandy gravels 1	2.2～0	1 800	1 024.6	1 254.6	1.310	1.170
XPS board	1.4～1.32	30	1 250.0	1 250.0	0.028	0.028
Sandy gravels 2	0～−1.8	1 800	1 024.6	1 254.6	1.310	1.170
Silty sand	−1.8～−3.8	1 400	1 275.5	1 464.1	0.790	0.840
Sandy gravels 3	−3.8～−15	1 800	1 024.6	1 254.6	1.310	1.170

Note: D is depth of soil layer.

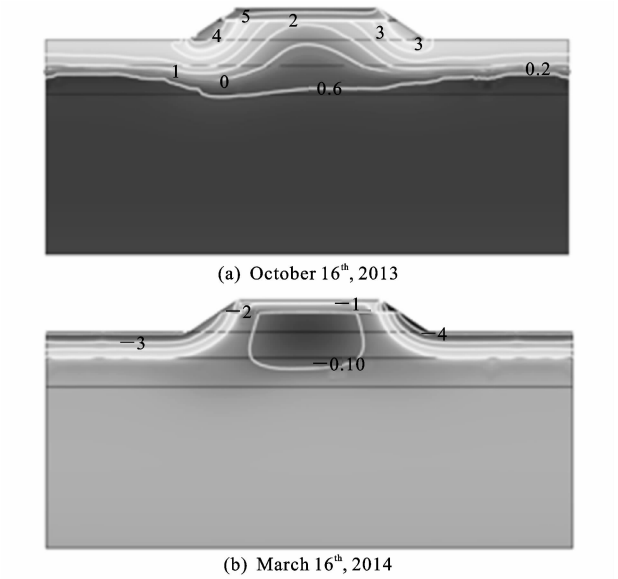

Fig. 7 Distribution characteristics of subgrade temperature field

图 7 路基温度场的分布特征

Tab. 2 Mean annual temperature and amplitude

表 2 相位与年平均温度 ℃

Position	T_0	A	φ
Subgrade center	1.38	4.09	1.86
Left side slope	1.22	8.00	2.33
Right side slope	0.19	7.84	2.32
Natural surface	−0.65	6.00	2.31

cording to Eq. (9) so that the stabilized ground temperature field could be regarded as initial value of natural foundation temperature. Then, with consideration for subgrade filling, the initial ground temperature of subgrade was the mean annual ground temperature of the foundation surface after 50 years.

Based on the established moisture-thermal coupling model of frozen soils, ground temperature distribution characteristics in October 16th of the second year and those in March 16th of the third year after the construction of roadbed are simulated, and the distribution characteristic of subgrade temperature field is shown in Fig. 8. The simulated and measured values for the thawing depth of the natural ground at different time are shown in Fig. 9. It can be seen that the simulated thawing depth is close to the measured value, and the error between simulated values and measured values is less than 0.3 m. Additionally, these results can prove the validity of the moisture-thermal coupling model.

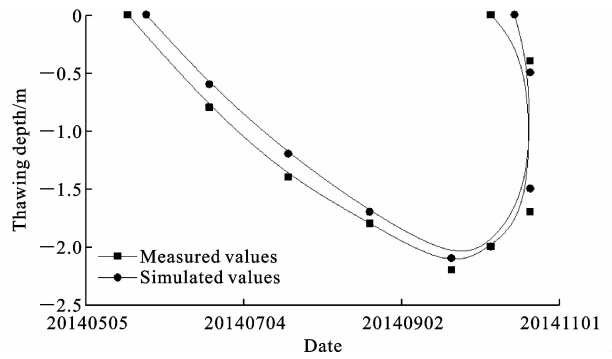

Fig. 8 Simulated and measured values for thawing depth of natural ground at different dates

图 8 天然地面不同时间的融化深度模拟值与监测值

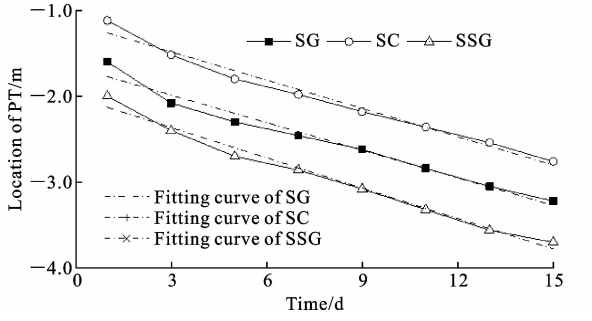

Fig. 9 Change laws of permafrost table (PT) of subgrade with different filling materials

图 9 不同填料情况下路基冻土上限的变化规律

3 Calculation model of permafrost table

3.1 Numerical calculation of permafrost table

Long-term deformation of subgrade in warm frozen soil regions is mainly caused by thaw settlement of frozen soils, while the main reason for subgrade thaw settlement is the decline of artificial permafrost table. In permafrost regions, the deterioration rate of artificial permafrost table is generally regarded as a referential index of subgrade thaw settlement. Therefore, by the moisture-heat coupling model, the paper calculated the impact degrees of different conditions on the decline of permafrost table, including different filling types, annual mean ground temperature, height of subgrade, laying location of XPS insulated board and climate warming. Tab. 3 shows the location of permafrost table at the subgrade center under different working conditions.

Taking the first working condition (different

Tab. 3　Change position of permafrost table of subgrade center under different working conditions with times

表 3　不同工况下路基中心冻土上限随时间的变化位置

Working condition year	CWC	Permafrost table changes/m							
		1 year	3 years	5 years	7 years	9 years	11 years	13 years	15 years
Filling type	SG	−1.60	−2.08	−2.30	−2.46	−2.62	−2.84	−3.05	−3.22
	SC	−1.00	−1.52	−1.80	−1.98	−2.18	−2.36	−2.54	−2.76
	SSG	−2.00	−2.40	−2.70	−2.86	−3.08	−3.32	−3.56	−3.70
Mean annual ground temperature	−0.5 ℃	−1.80	−2.09	−2.28	−2.45	−2.63	−2.90	−3.10	−3.30
	−1.0 ℃	−1.60	−2.08	−2.30	−2.46	−2.62	−2.84	−3.05	−3.22
	−1.5 ℃	−1.84	−2.1	−2.30	−2.44	−2.59	−2.78	2.99	−3.20
Subgrade height	2.2 m	−1.60	−2.08	−2.30	−2.46	−2.62	−2.84	−3.05	−3.22
	2.6 m	−1.72	−2.12	−2.29	−2.45	−2.61	−2.80	−3.00	−3.13
	3.0 m	−1.84	−2.07	−2.26	−2.42	−2.63	−2.78	−2.89	−3.00
XPS insulated board position	0.4 m	−1.90	−2.22	−2.40	−2.56	−2.72	−2.96	−3.20	−3.43
	0.8 m	−1.60	−2.08	−2.30	−2.46	−2.62	−2.84	−3.05	−3.22
	1.2 m	−1.28	−1.90	−2.20	−2.37	−2.56	−2.76	−2.95	−3.13
Climate warming rate	0	−1.55	−1.90	−2.00	−2.10	−2.15	−2.16	−2.22	−2.23
	0.052 ℃ per year	−1.60	−2.08	−2.30	−2.46	−2.62	−2.84	−3.05	−3.22

Note: CWC is stand for classification of each working condition; SSG is stand for silty soil with gravel; SG is stand for sandy gravels; SC is stand for silty clay.

Tab. 4　Fitting formulas of permafrost table change of subgrade with three different fillers

表 4　三种不同填料的路基的冻土上限变化拟合公式

Subgrade filling	Fitting formula	Correlation coefficient
SG(1-1)	$P=-1.666-0.107t$	0.969
SC(1-2)	$P=-1.153-0.11t$	0.978
SSG(1-3)	$P=-2.011-0.118t$	0.982

Note: P is stand for position of permafrost table.

filling types) as an example, Fig. 9 indicates the linear fit of changing laws of permafrost table of subgrades with different fillings over time. The fitting formulas of permafrost table of subgrades with different fillings are shown in Tab. 4.

3.2　Establishment and verification of the calculation model

With the consideration of different impact degrees on permafrost table under different working conditions, importance of the five indexes (filling type, annual mean ground temperature, height of subgrade, laying locations of XPS insulated board and climate warming) was analyzed at first. The paper applied the entropy weight method to calculate the weight of the five indexes. The specific calculating process is as follows:

(1) Standardizing treatment

The five given indexes $X_j(j=1, 2, \cdots, 5)$ shoud be standardized, among which $X_j=\{x_1, x_2, \cdots, x_m\}$. The standardized values of the five indexes Y_j

$$Y_j=\frac{X_j-\min(X_j)}{\max(X_j)-\min(X_j)} \tag{10}$$

(2) Information entropy of each index

According to the definition of information entropy from the theory of information, the information entropy e_j of a data set data is

$$e_j=-\frac{1}{\ln(m)}\sum_{i=1}^{m}p_{ij}\ln(p_{ij}) \tag{11}$$

$$p_{ij}=\frac{Y_{ij}}{\sum_{i=1}^{m}Y_{ij}} \quad 0\leqslant p_{ij}\leqslant 1 \tag{12}$$

where $p_{ij}(i=1, 2, \cdots, m)$ is weight of individual index; Y_{ij} is standardized values of individual index of the five indexes.

(3) Weight of each index

In accordance with the calculation formula of information entropy, the information entropy of the five indexes is e_1, $e_2, \cdots, e_5$ and the avail value of the index $d_j=1-e_j$. Weights w_j of the five indexes are calculated by information entropy

$$w_j=\frac{d_j}{\sum_{j=1}^{5}d_j} \tag{13}$$

By using MATLAB software, weights of filling types, annual mean ground temperature,

height of subgrade, laying locations of XPS insulated board and climate warming, were calculated as 0.36, 0.01, 0.02, 0.04, 0.57, respectively. From the data above, filling type and climate warming have a significant effect on the decline of permafrost table. Therefore, by considering the two most significant factors that affecting the decline of permafrost table as well as on the basis of the conclusion that permafrost table increases linearly with time under different working conditions, the fitting model of permafrost table is

$$p=\lambda_0+\lambda_1 F+\lambda_2 R+\lambda_3 \ln(t_1) \quad (14)$$

where p refers to permafrost table; F refers to subgrade fillings; R refers to warming temperatures which is 0.052 ℃ per year; t_1 refers to time (year); $\lambda_k(k=0,1,2,3)$ is coefficient.

By adopting MATLAB statistical tool, the multivariate linear regression is conducted on the two major factors affecting the decline of permafrost table. The calculation model of permafrost table is

$$p=-0.967-0.217F-0.235R+0.509\ln(t) \quad (15)$$

To verify the calculation model of the permafrost table of XPS insulated board subgrade, the measured values of reference were used to compare with the calculated values of the model[22-23]. Fig. 10 shows that the measured and calculated values have a higher degree of agreement, and the error between measured and calculated values was kept within 0.06 m. Therefore, the calculation model of permafrost table change can reflect the degradation trend and the magnitude of permafrost table.

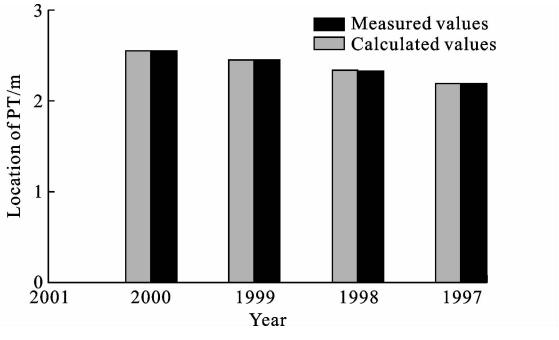

Fig. 10 Measured and calculated values of PT of XPS insulated board subgrade

图 10 XPS 保温板路基冻土上限的监测值与计算值

4 Conclusions

(1) By comparing the simulated and the measured temperature fields, it has been verified that the moisture-heat coupling model is able to simulate exactly the changing laws of temperature field of XPS insulated board subgrade in warm permafrost regions.

(2) The temperature on the left side of subgrade within a certain range is higher than that on the right side within the corresponding range both in cold and warm seasons, which proves that after building the embankment, ground temperature distribution of subgrade varies greatly between the south-faced slope and the north-faced slope as a result of slope orientations and different boundary conditions.

(3) The artificial permafrost table is lifted with value of 60 cm at the early stage of subgrade completion. Then, the artificial permafrost table decreases 10 cm per year, but the temperature of the underlying permafrost has an increasing tendency year by year all the time. This implies that the changes of artificial permafrost table will consume the cold-storing quantities of underlying permafrost.

(4) The artificial permafrost table of subgrade increases linearly with time under different conditions. Moreover, filling type and climate warming are two major factors affecting the decline of permafrost table, and the calculation model of permafrost table is established. Conclusively, the calculation model in permafrost regions serves as a favorable reference for traffic departments to carry out prediction on long-term life of XPS insulated board subgrade in future.

(5) Ground temperature of XPS insulated subgrade in warm permafrost regions should be monitored continuously, and the calculation model of permafrost table of XPS insulated board subgrade in warm permafrost regions should be further improved by comparing the calculated values with the measured values.

Acknowledgements

This research is supported by the National Natural Science Foundation of China (No. 41271072 and 51378057); Science and Technology Project of Qinghai Province (No. 2013-J-770); Science and Technology Project of Shenshuo Railway Branch (No. 2015-10).

References:

[1] TAI Bo-wen, FANG Jian-hong, LIU Lei, et al. Temperature monitoring of the XPS board insulated subgrade along the newly constructed Gonghe-Yushu Highway in permafrost regions[J]. Sciences in Cold and Arid Regions, 2015, 7(5): 520-527.

[2] SHENG Yu, WEN Zhi, MA Wei. Preliminary analysis on insulation treatment of embankment at Beiluhe Test Section of Qinghai-Tibet Railway[J]. Chinese Journal of Rock Mechanics and Engineering, 2003, 22(S2): 2659-2663.

[3] WEN Zhi, SHENG Yu, MA Wei, et al. Evaluation of EPS application to embankment of Qinghai-Tibetan Railway[J]. Cold Regions Science and Technology, 2005, 41(3): 235 -247.

[4] DONG Yuan-hong, ZHU Dong-peng, ZHANG Hui-jian, et al. Mechanical properties of XPS thermal insulation board applied in permafrost embankment[J]. China Journal of Highway and Transport, 2015, 28(12): 64-68.

[5] HOU Shu-guang, BIAN Jiang, WANG Shuang-jie. Numerical simulation of thermal state EPS insulation roadbed in permafrost region[J]. Journal of Nanjing University of Technology, 2007, 29(1): 27-31.

[6] CHEN Ji, FENG Zi-liang, SHENG Yu, et al. Permafrost along National Highway 214 and its engineering geological condition evaluation[J]. Journal of Glaciology and Geocryology, 2014, 36(4): 790-801.

[7] LIU Ge, WANG Shuang-jie, YUAN Kun, et al. Adaptability and optimization of permafrost embankment structure under scale effect[J]. China Journal of Highway and Transport, 2015, 28(12): 17-25.

[8] WANG Shuang-jie, LIU Ge, YE Li, et al. Research on control countermeasures of thermal effect of wide embankment in permafrost regions[J]. China Journal of Highway and Transport, 2015, 28(12): 26-32.

[9] CHENG Guo-dong, ZHANG Jian-ming, SHENG Yu, et al. Principle of thermal insulation for permafrost protection[J]. Cold Regions Science and Technology, 2004, 40(1/2): 71-79.

[10] MA Wei, CHENG Guo-dong, WU Qing-bai. Preliminary study on technology of cooling foundation in permafrost regions[J]. Journal of Glaciology and Geocryology, 2002, 24(5): 579-587.

[11] NIU Fu-jun, LIU Ming-hao, CHENG Guo-dong, et al. Long-term thermal regimes of the Qinghai-Tibet Railway embankments in permafrost regions[J]. Science China Earth Sciences, 2015, 58(9): 1669-1676.

[12] ZHANG Ming-yi, LI Shuang-yang, GAO Zhi-hua, et al. Nonlinear analysis of the temperature field of the embankment with crushed-rock revetment and insulation along the Qinghai-Tibetan Railway[J]. Journal of Glaciology and Geocryology, 2007, 29(2): 306-314.

[13] MA Wei, MU Yan-hu, LI Guo-yu, et al. Responses of embankment thermal regime to engineering activities and climate change along the Qinghai-Tibet Railway [J]. Scientia Sinica Terrae, 2013, 43(3): 478-489.

[14] LIU Zhi-qiang, LAI Yuan-ming, ZHANG Xue-fu, et al. Numerical analysis of the ventilated embankment with thermal insulation layer in Qing-Tibetan Railway[J]. Chinese Journal of Rock Mechanics and Engineering, 2005, 24(14): 2537-2543.

[15] LIU Zhi-qiang, LAI Yuan-ming. Numerical analysis for the ventilated embankment with thermal insulation layer in Qing-Tibetan railway[J]. Cold Regions Science and Technology, 2005, 42(3): 177-184.

[16] LAI Yuan-ming, ZHANG Lu-xin, ZHANG Shu-jian, et al. Cooling effect of ripped-stone embankments on Qinghai-Tibet Railway under climatic warming[J]. Chinese Science Bulletin, 2003, 48(6): 598-604.

[17] LIU Jian-kun, TIAN Ya-hu. Numerical studies for the thermal regime of a roadbed with insulation on permafrost[J]. Cold Regions Science and Technology, 2002, 35(1): 1-13.

[18] TAO Wen-quan. Heat transfer[M]. Xi'an: Northwestern Polytechnical University Press, 2006.

[19] XU Xue-zu, DENG You-sheng. Experimental research on moisture migration in permafrost[M]. Beijing: Science Press, 1991.

[20] XU Xue-zu, WANG Jia-cheng, ZHANG Li-xin. Physics of frozen soils[M]. Beijing: Science Press, 2001.

[21] BAI Qing-bo, LI Xu, TIAN Ya-hu, et al. Equations and numerical simulation for coupled water and heat transfer in frozen soil[J]. Chinese Journal of Geotechnical Engineering, 2015, 37(S2): 131-136.

[22] SHENG Yu, WEN Zhi, MA Wei, et al. Long-term evaluations of insulated road in the Qinghai-Tibetan Plateau[J]. Cold Regions Science and Technology, 2006, 45(1): 23-30.

[23] WEN Zhi, SHENG Yu, MA Wei, et al. Analysis on effect of permafrost protection by two-phase closed thermosyphon and insulation jointly in permafrost regions[J]. Cold Regions Science and Technology, 2005, 43(3): 150-163.